

$V_{g,t} = -4$  V. The mobility of the electrons can also be deduced from the transconductance of the FET. In the linear regime, it is given by  $dI/dV_g = \mu(CL^{-2})V_{ds}$ . From Figure 4b, we get  $dI/dV_g = 9.7 \times 10^{-10} \text{ A V}^{-1}$  at  $V_{ds} = 10$  mV, corresponding to an electron mobility of  $71 \text{ cm}^2 \text{ V}^{-1} \text{ s}^{-1}$ .

In summary, high-quality indium oxide nanowires were synthesized using a laser ablation technique, and their composition and single-crystalline structures were confirmed using XRD, TEM, and SAED. Precise control over the nanowire diameter was achieved by using monodispersed gold clusters as the catalytic nanoparticles. The growth can be explained by the VLS mechanism. FETs were also fabricated based on these nanowires. Detailed electrical measurements confirmed that the indium oxide nanowires were n-type semiconductors, and the on/off ratio of the field effect transistor can reach up to 1000. We believe these nanowires could be used as active sensing materials and also building blocks for nanoelectronics.

### Experimental

Si/SiO<sub>2</sub> substrates were cleaned in acetone and isopropanol. For growth with thin gold films as the catalyst, the substrates were coated with 20 Å Au using a Temescal e-beam evaporator, followed by baking in Ar atmosphere for half an hour to break the Au films into nanoparticles. For growth with nanoclusters as the catalyst, the substrates were coated with a layer of gold clusters (Ted Pella). Three kinds of clusters with diameters of  $10 \pm 1.5$  nm,  $20 \pm 2.0$  nm,  $30 \pm 3.0$  nm were used, and atomic force microscopy (Digital Instruments Dimension 3100) was performed to confirm these nanoclusters distributed uniformly across the surface. The substrates were loaded into a quartz tube at the downstream end of a furnace, and an InAs (Alfa Aesar, 99.999 %) target was placed at the upper stream of the furnace. The system was first pumped to a base pressure below 1 millitorr, and then Ar mixed with 0.02 % O<sub>2</sub> was flown through the system at a rate of 150 sccm, while the InAs target was ablated to supply the indium vapor. During the laser ablation process, the chamber was maintained at 220 torr, 770 °C. A pulsed Nd:YAG laser (Continuum) ( $L = 532$  nm) with repetition rate of 10 Hz, and a pulse power of 1.0 W was used. The typical reaction time used was about 35 min. After the furnace cooled down to room temperature, light gray materials were found on the surface of the substrate.

The crystal structure of the nanowires was characterized using XRD (Rigaku RV-200) and SAED (Phillips, 420 operated at 120 Kev). The nanowire diameters were usually determined from TEM (Phillips, 420 operated at 120 Kev) and the lengths were measured from SEM (Phillips XL30 operated at 15 Kev) images.

For electronic transport studies In<sub>2</sub>O<sub>3</sub> nanowires of 10 nm in diameter were sonicated for 1 h in isopropanol, and then several drops were deposited onto a degenerately doped silicon wafer covered with 500 nm SiO<sub>2</sub>. Photolithography was performed, followed by evaporating Ti/Au to contact both ends of the nanowires. Devices with a single In<sub>2</sub>O<sub>3</sub> nanowire between the source and drain electrodes were chosen for further studies after a thorough SEM inspection. The electrical measurements were carried out using a semiconductor parameter analyzer (Agilent 4156B).

Received: July 25, 2002  
Final version: November 11, 2002

- [1] Y. Wu, P. Yang, *Chem. Mater.* **2000**, *12*, 605.  
[2] M. H. Huang, Y. Wu, H. Feick, N. Tran, E. Weber, P. Yang, *Adv. Mater.* **2001**, *13*, 113.  
[3] J. Kong, C. Zhou, A. Mørpurgo, H. T. Soh, C. F. Quate, C. Marcus, H. Dai, *Appl. Phys. A* **1999**, *69*, 305.  
[4] Y. Cui, L. J. Lauhon, M. S. Gudiksen, J. Wang, C. M. Lieber, *Appl. Phys. Lett.* **2001**, *78*, 2214.  
[5] J. T. Hu, T. W. Odom, C. M. Lieber, *Acc. Chem. Res.* **1999**, *32*, 435.  
[6] X. Duan, C. M. Lieber, *J. Am. Chem. Soc.* **2000**, *122*, 188.  
[7] A. M. Morales, C. M. Lieber, *Science* **1998**, *279*, 208.  
[8] M. J. Zheng, L. D. Zhang, G. H. Li, X. Y. Zhang, X. F. Wang, *Appl. Phys. Lett.* **2001**, *79*, 839.

- [9] a) Y. Huang, X. Duan, Y. Cui, C. M. Lieber, *Nano Lett.* **2002**, *2*, 101. b) C. C. Chen, C. C. Yeh, *Adv. Mater.* **2000**, *12*, 738. c) J. Zhu, S. Fan, *J. Mater. Res.* **1999**, *14*, 1175. d) J. Kim, H. So, J. Park, J. Kim, J. Kim, C. Lee, S. Lyu, *Appl. Phys. Lett.* **2002**, *80*, 3548.  
[10] X. F. Duan, C. M. Lieber, *Adv. Mater.* **2000**, *12*, 298.  
[11] Y. Huang, X. Duan, Y. Cui, L. Lauhon, K. Kim, C. M. Lieber, *Science* **2001**, *294*, 1313.  
[12] M. Huang, S. Mao, H. Feick, H. Yan, Y. Wu, H. Kind, E. Weber, R. Russo, P. Yang, *Science* **2001**, *292*, 1897.  
[13] K. Sreenivas, T. S. Rao, A. Mansingh, *J. Appl. Phys.* **1985**, *57*, 384.  
[14] Y. Shigesato, S. Takaki, T. Haranoh, *J. Appl. Phys.* **1992**, *71*, 3356.  
[15] a) J. Tamaki, C. Naruo, Y. Yamamoto, M. Mastuoka, *Sens. Actuators B* **2002**, *83*, 190. b) D. E. Williams, *Sens. Actuators B* **1999**, *57*, 1. c) M. Liess, *Thin Solid Films* **2002**, *410*, 183.  
[16] X. S. Peng, G. W. Meng, J. Zhang, X. F. Wang, Y. W. Wang, C. Z. Wang, L. D. Zhang, *J. Mater. Chem.* **2002**, *12*, 1602.  
[17] Z. W. Pan, Z. R. Dai, Z. R. Wang, *Science* **2001**, *291*, 1947.  
[18] M. S. Gudiksen, J. Wang, C. M. Lieber, *J. Phys. Chem. B* **2001**, *105*, 4062.  
[19] R. W. G. Wyckoff, *Crystal Structures*, Interscience, New York **1968**.  
[20] S. J. Tans, A. R. M. Verschueren, C. Dekker, *Nature* **1998**, *393*, 49.  
[21] R. Martel, T. Schmidt, H. R. Shea, T. Hertel, P. Avouris, *Appl. Phys. Lett.* **1998**, *73*, 2447.  
[22] C. Zhou, J. Kong, E. Yenilmez, H. Dai, *Science* **2000**, *290*, 1552.

### An Unusual Electrochromic Device Based on a New Low-Bandgap Conjugated Polymer\*\*

By Hong Meng, Derald Tucker, Sterling Chaffins, Yongsheng Chen, Roger Helgeson, Bruce Dunn, and Fred Wudl\*

Over the past few years, electrochromic devices (ECDs) using electrochemically active conjugated polymers have been widely investigated.<sup>[1]</sup> Interest in these materials is due to their advantageous properties such as low fabrication cost, processibility, and dynamic, color-tunable “smart windows”.<sup>[1,2]</sup> Conjugated polyheterocyclic polymers, such as polyanilines, polypyridines, polypyrroles, polythiophenes, and in particular, poly(3,4-ethylenedioxythiophene) (PEDOT) and its derivatives have been studied as electrochromic materials.<sup>[3,4]</sup> These materials provide color changes within the visible spectrum, and some exhibit electrochromicity, changing from a transparent doped state to a colored neutral state.<sup>[4]</sup> As a decrease of absorption in the transparent doped state is accompanied by an increase of absorption in the infrared region, the application of a conducting-polymer-based “smart window” can be extended to infrared ranges.<sup>[5]</sup> Infrared modulation devices show great potential in devices such as a vari-

[\*] Prof. F. Wudl, Dr H. Meng, Dr. S. Chaffins, Dr. Y. Chen, Dr. R. Helgeson  
Department of Chemistry and Biochemistry  
Exotic Materials Institute  
University of California at Los Angeles  
Los Angeles, CA 90095-1569 (USA)  
E-mail: wudl@chem.ucla.edu  
Dr. D. Tucker, Prof. B. Dunn  
Department of Materials Science and Engineering  
Exotic Materials Institute  
University of California at Los Angeles  
Los Angeles, CA 90095-1569 (USA)

[\*\*] We thank the U.S. Air Force Office of Scientific Research for support through F49620-00-1-0103 and a MURI from the U.S. Army Research Office through DAAD19-99-1-0316.

---

able optical attenuator for optical information technology,<sup>[5]</sup> infrared camouflage for warfare in low-light environments, and thermal emission detectors for aerospace applications.<sup>[6]</sup> Such devices will be cost-effective, lightweight, and can even be designed to be flexible.<sup>[7]</sup>

Low-bandgap conjugated polymers possess a variety of intrinsic properties such as transparency in the neutral state, stability in electrochemical p- and n-doping processes, and absorption in the infrared range during the doping process.<sup>[8]</sup> Based on these characteristics, such polymers are envisioned as unique electrochromic materials.

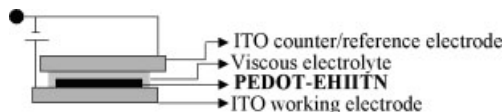


Fig. 3. Schematic structure of transmittance electrochromic device (ECD).

Figure 4 exhibits spectroelectrochemical UV-vis-NIR transmittance spectra of PEDOT-EHIITN ECD under various applied voltages. The films were translucent without applying a

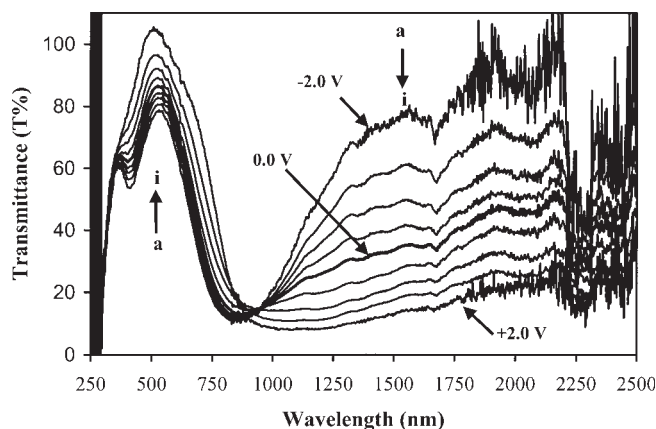


Fig. 4. Spectroelectrochemical UV-vis-NIR transmittance spectra of PEDOT-EHIITN ECD under different applied voltages: a)  $-2.0$  V. b)  $-1.5$  V. c)  $-1.0$  V. d)  $-0.5$  V. e)  $0$  V. f)  $+0.5$  V. g)  $+1.0$  V. h)  $+1.5$  V. i)  $+2.0$  V.

voltage because the easily oxidized polymer is partially doped by electron transfer from the indium tin oxide (ITO) electrode (in the presence of electrolyte).<sup>[14]</sup> When a positive voltage was applied, the polymer film was further oxidized and the device became more transparent, as the absorption maximum was shifted from 850 nm into the mid-IR region. When a negative voltage was applied, the absorption spectrum became narrower, with the maximum peak slightly blue-shifted from 850 nm. Negative voltages can restore the neutral polymer with its characteristic blue color. These spectral changes can be observed many times on potential cycling, without any noticeable degradation. Interestingly, unlike other ECDs,<sup>[1,9,13]</sup> this low-bandgap conjugated-polymer-based ECD showed significant electronic absorption changes in the near- and mid-IR wavelengths, but few in the visible range. Under different applied voltages, the ECD remains transparent and there are slight absorbance changes in the visible range of 400 nm to 600 nm, corresponding to 3.1 eV to 2.1 eV, respectively (Fig. 4). On the other hand, the changes in near-IR and mid-IR range are much more profound. A possible explanation for this phenomenon may reside with the intrinsic characteristics of the low-bandgap conducting polymer, which lacks absorbance in the visible range. The n-doping process of PEDOT-EHIITN did not shift the absorbance into the NIR area because reduction very likely occurred at the imide side group, which forms a localized imide anion radicals.<sup>[15]</sup>

It is clearly seen from the transmittance spectra in Figure 5 that there is a large contrast between the fully oxidized

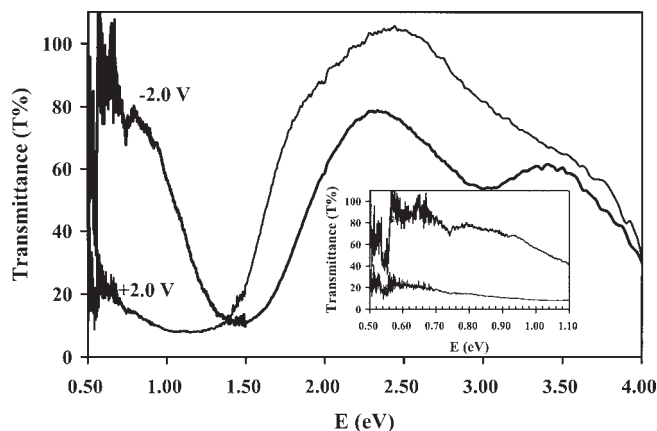


Fig. 5. UV-vis-NIR transmittance spectra of PEDOT-EHIITN ECD in fully oxidized ( $+2.0$  V) and reduced forms ( $-2.0$  V). Inset: Expansion of the 0.5–1.1 eV region.

( $+2.0$  V) and reduced ( $-2.0$  V) states as  $\Delta T\%$  is around 60–80 % in the wide range of 1.10 eV to 0.58 eV, corresponding to 1130 nm to 2140 nm, respectively. The device is transparent during the operation: the ECD is unchanged at ca. 1.4 eV in the visible range and the absorption peak between 750–1000 nm (1.65–1.24 eV) loses very little intensity.

The switching time was determined by monitoring the absorption intensity changes at 1500 nm through switching the applied voltage between  $-2.0$  V and  $+2.0$  V (Fig. 6). The switching time for PEDOT-EHIITN was experimentally determined to be 4.8 s. Our result is comparable with previously fabricated ECDs utilizing active layers of PEDOT (2 s) and polythiophenes (4 s).<sup>[16]</sup>

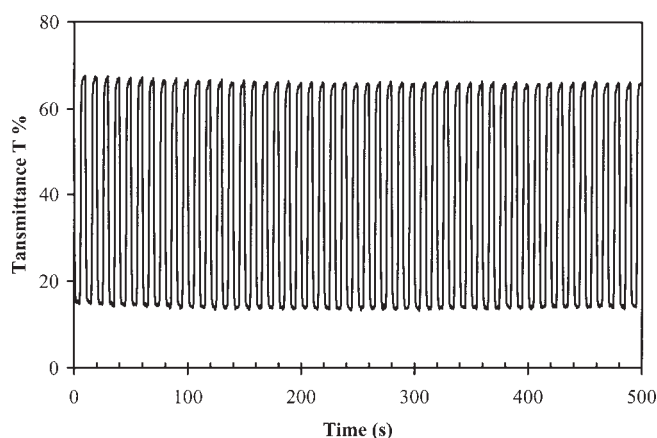


Fig. 6. Optical switching for PEDOT-EHIITN ECD monitored at 1500 nm with potential stepped between  $-2.0$  V and  $+2.0$  V.

In summary, a new low-bandgap conjugated polymer has been synthesized and its properties have been investigated. Our experimental results show that this transparent, processable, low-bandgap conjugated polymer demonstrated an electrochromic behavior specific to the infrared range. The absence of electrochromism in the visible range may permit this unique polymer to be used in specific infrared device applications.

## Experimental

Unless stated otherwise, all commercial chemicals and solvents were used as received without further purification. Reagent chemicals were purchased either from Aldrich or Fisher Chemical Co, unless otherwise stated. All new compounds were characterized by  $^1\text{H}$  and  $^{13}\text{C}$  NMR spectroscopy, mass spectrometry, and elemental analysis. NMR spectra were taken on a Bruker ARX 400 spectrometer. All chemical shifts were reported relative to tetramethylsilane (TMS). UV-vis-NIR spectroelectrochemistry was carried out on a Shimadzu UV 3101PC UV-vis-NIR spectrophotometer. Melting points were measured using a capillary melting point apparatus (MelTemp from Laboratory Devices) and were uncorrected. Elemental analysis results were obtained from Desert Analytics Co. Light-scattering measurements were performed at a concentration of  $8\text{ mg mL}^{-1}$  with Microtrac Ultrafine Particle Analyzer (Leeds & Northrup). Cyclic voltammetry (CV) and differential pulse voltammetry (DPV) were performed on a BAS 100B Electrochemical Analyzer in a three-electrode cell in a solution of  $\text{Bu}_4\text{NBF}_4$  (0.1 M) in acetonitrile at a scan rate of  $50\text{ mV s}^{-1}$ . The polymer films were coated on a glassy carbon disc electrode ( $0.5\text{ cm}^2$ ) by casting the polymer solutions onto the electrode and then drying in vacuum. A Pt wire was used as the counter electrode and an  $\text{Ag}/\text{AgNO}_3$  (0.1 M) electrode was used as the reference electrode. Its potential was corrected to the saturated calomel electrode (SCE) by measuring the ferrocene/ferrocenium couple in this system (0.31 V vs. SCE). For electrochromic device characterization, the top ITO glass slide acts as both the counter and the reference electrodes and the bottom ITO glass slide as a working electrode.

**Electrochromic Device Fabrication:** The polymer films were spin-coated onto ITO-coated glass plates ( $50\ \Omega/\square$ ). The film thickness was measured by a Dektak 8 profilometer. The viscous electrolyte was lithium perchlorate-plasticized by mixing with propylene carbonate and poly(methyl methacrylate) in acetonitrile (the ratio of the composition of  $\text{LiClO}_4/\text{PC}/\text{PMMA}/\text{CH}_3\text{CN}$  is 3:20:7:70 by weight). The mixture was stirred overnight at room temperature under an argon atmosphere.

**2,9-Dibromo-benzo[*c*]thiophene-*N*-2'-ethylhexyl-4,5-dicarboxylimide (EHI-DBrITN):** At  $0\text{--}5\text{ }^\circ\text{C}$  under an argon atmosphere, NBS powder (1.28 g, 7.2 mmol) was added slowly to a stirred solution of benzo[*c*]thiophene-*N*-2'-ethylhexyl-4,5-dicarboxylic imide (EHIITN)[11] (1.10 g, 3.5 mmol) dissolved in a mixture of chloroform (50 mL) and acetic acid (50 mL). The mixture was stirred for 24 h at room temperature and then refluxed for an additional 2 h. The mixture was quenched with water, the organic layer was separated, and the water layer was extracted with chloroform (10 mL  $\times$  3). The combined chloroform extracts were neutralized with 5% sodium bicarbonate solution and then washed again with distilled water. After drying with anhydrous magnesium sulfate and filtering, the solvent was evaporated and the residue was purified by column chromatography using methylene chloride: hexane (2:1) as eluent on silica to afford 1.3 g of a light yellow solid (78%). mp,  $173\text{--}175\text{ }^\circ\text{C}$ ;  $^1\text{H}$  NMR ( $\text{CDCl}_3$ , 400 MHz):  $\delta$  8.00 ppm (s, 2H, ArH), 3.63 ppm (d, 2H,  $J=7.2\text{ Hz}$ ,  $-\text{NCH}_2$ ), 1.88 ppm (m, 1H,  $-\text{NCH}_2\text{CH}$ ), 1.29–1.36 ppm (m, 8H,  $-\text{CH}_2$ ), 0.86–0.92 ppm (m, 6H,  $-\text{CH}_3$ ).  $^{13}\text{C}$  NMR ( $\text{CDCl}_3$ , 400 MHz):  $\delta$  167.4, 137.9, 127.2, 118.5, 109.9, 42.51, 38.13, 30.55, 28.50, 23.90, 23.01, 14.07, 10.44 ppm. Electron impact (EI) mass spectrometry (MS)  $m/z$  (%): 360 (100,  $\text{M}^+ - \text{C}_8\text{H}_{17}$ ), 471 (45,  $\text{M}^+ - 2$ ), 473 (80,  $\text{M}^+$ ), 475 (45,  $\text{M}^+ + 2$ ). Anal. Calcd. for  $\text{C}_{18}\text{H}_{19}\text{Br}_2\text{NO}_2$ : C, 45.86; H, 4.07; Br, 33.80; N, 2.97; S, 6.77. Found: C, 46.38; H, 4.08; Br, 32.16; N, 3.31; S, 6.47.

**2,5-Bis(tributylstannyl)-3,4-ethylenedioxythiophene:** This compound was prepared according to the literature procedure [12]. Colorless liquid; bp,  $140\text{ }^\circ\text{C}/0.15\text{ mmHg}$ .  $^1\text{H}$  NMR ( $\text{CDCl}_3$ , 400 MHz):  $\delta$  4.11 ppm (s, 4H,  $-\text{OCH}_2$ ), 1.52–1.58 ppm (m, 12H,  $-\text{SnCH}_2$ ), 1.30–1.36 ppm (m, 12H,  $-\text{CH}_2$ ), 1.06–1.10 ppm (m, 12H,  $-\text{CH}_3$ ), 0.87–0.91 ppm (t, 18H,  $J=7.2\text{ Hz}$ ,  $-\text{CH}_3$ ).  $^{13}\text{C}$  NMR ( $\text{CDCl}_3$ ):  $\delta$  148.3, 115.8, 64.65, 28.93, 27.23, 13.72, 10.51 ppm. EI, MS  $m/z$  (%): 720 (5,  $\text{M}^+$ ), 663 (100,  $\text{M}^+ - \text{C}_4\text{H}_9$ ), 473 (35,  $\text{M}^+ - \text{SnBu}_4$ ), 291 (18,  $\text{M}^+ - 473$ ). Anal. Calcd. for  $\text{C}_{30}\text{H}_{58}\text{O}_2\text{SSn}_2$ : C, 50.03; H, 8.12; S, 4.45; Sn, 32.96. Found: C, 50.37; H, 8.29; S, 4.23; Sn, 32.46.

**Poly(3,4-ethylenedioxythiophene)-benzo[*c*]thiophene-*N*-2'-ethylhexyl-4,5-dicarboxylic imide (PEDOT-EHIITN):** 2,5-Bis(tributylstannyl)-3,4-ethylenedioxythiophene (1.468 g, 2.04 mmol) and 2,5-dibromo-benzo[*c*]thiophene-*N*-2'-ethylhexyl-4,5-dicarboxylic imide (DiBrEHIITN) (0.946 g, 2.00 mmol) were dissolved in 20 mL of tetrahydrofuran (THF) under an argon atmosphere. A catalytic amount of dichlorobis(triphenylphosphine)palladium(II) [ $\text{PdCl}_2(\text{PPh}_3)_2$ ] (30 mg, 0.04 mmol) was added and the mixture was refluxed for 48 h. After cooling, the reaction mixture was poured into methanol (100 mL). The black precipitate was then collected by centrifugation. After washing several times with methanol, the crude polymer was further purified by redissolving in chloroform and repeatedly precipitated with methanol to afford a blue-black solid powder. The polymer was extracted with methanol, acetone, THF, and finally with chloroform using a Soxhlet extractor. The polymer was further purified by dissolving it in chloroform and precipitating it with methanol, followed by centrifugation. After drying under vacuum overnight at  $40\text{ }^\circ\text{C}$ , the purified

polymer was obtained as deep blue powder (650 mg, yield: 71%).  $^1\text{H}$  NMR ( $\text{CDCl}_3$ , 400 MHz):  $\delta$  8.64–7.02 ppm (br, 2H, ArH), 3.51–4.82 ppm (br, 6H,  $\text{OCH}_2$ ,  $-\text{NCH}_2$ ), 0.85–1.88 ppm (br, 15 H,  $-\text{CH}_2$ ,  $-\text{CH}_3$ ).  $^{13}\text{C}$  NMR ( $\text{CDCl}_3$ ):  $\delta$  167.7, 138.3, 134.2, 128.4, 126.1, 118.7, 110.5, 65.40, 42.12, 38.20, 30.57, 28.62, 23.90, 23.02, 14.13, 10.43 ppm. Anal. Calcd. for  $\text{C}_{24}\text{H}_{23}\text{NO}_4\text{S}_2$ : C, 63.55; H, 5.11; N, 3.09; S, 14.14. Found: C, 60.56; H, 5.66; N, 3.13; S, 12.92. The molecular weight  $\bar{M}_w$  of the polymer was determined to be  $47000\text{ g mol}^{-1}$ , determined using a light-scattering measurement.

Received: September 6, 2002  
Final version: October 24, 2002

- a) D. R. Rosseinsky, R. J. Mortimer, *Adv. Mater.* **2001**, *13*, 783. b) M.-A. De Paoli, G. Casalbore-Miceli, E. M. Giroto, W. A. Gazotti, *Electrochim. Acta* **1999**, *44*, 2983.
- M. Pomerantz, in *Handbook of Conducting Polymers* (Eds: T. A. Skotheim, R. L. Elsenbaumer, J. R. Reynolds), 2nd ed., Marcel Dekker, New York **1998**, Ch. 5.
- a) B. C. Thompson, P. Schottland, K. Zong, J. R. Reynolds, *Chem. Mater.* **2000**, *12*, 1563. b) R. J. Mortimer, *Electrochim. Acta* **1999**, *44*, 2971.
- a) I. Schwendeman, J. Hwang, D. M. Welsh, D. B. Tanner, J. R. Reynolds, *Adv. Mater.* **2001**, *13*, 634. b) P. Schottland, K. Zong, G. L. Gaupp, B. C. Thompson, C. A. Thomas, I. Giurgiu, R. Hickman, K. A. Abboud, J. R. Reynolds, *Macromolecules* **2000**, *33*, 7051.
- a) M. McDonagh, S. R. Bayly, D. J. Riley, M. D. Ward, J. A. McCleverty, M. A. Cowin, C. N. Morgan, R. Varrazza, R. V. Penty, I. H. White, *Chem. Mater.* **2000**, *12*, 2523.
- a) P. Chandrasekhar, G. C. Birur, P. Stevens, S. Rawel, E. A. Pierson, K. L. Miller, *Synth. Met.* **2001**, *119*, 293. b) P. Chandrasekhar, *US Patent* 5995273, **1999**.
- A. Bessière, C. Marcel, M. Morcrette, J. M. Tarascon, V. Lucas, B. Viana, N. Baffier, *J. Appl. Phys.* **2002**, *91*, 158.
- J. Roncali, *Chem. Rev.* **1997**, *97*, 173.
- a) J. P. Ferraris, C. Henderson, D. Torres, D. Meeker, *Synth. Met.* **1995**, *72*, 145. b) C. Arbizzani, M. G. Cerroni, M. Mastragostino, *Sol. Energy Mater. Sol. Cells* **1999**, *56*, 205.
- a) Q. T. Zhang, J. M. Tour, *J. Am. Chem. Soc.* **1998**, *120*, 5355. b) S. Akoudad, J. Roncali, *Chem. Commun.* **1998**, 2081.
- H. Meng, F. Wudl, *Macromolecules* **2001**, *34*, 1810.
- Z. Bao, W. K. Chan, L. Yu, *J. Am. Chem. Soc.* **1995**, *117*, 12426.
- S. A. Sapp, G. A. Sotzing, J. R. Reynolds, *Chem. Mater.* **1998**, *10*, 2101.
- Physical Chemistry* (Ed: P. W. Atkins), 4th ed., Oxford University Press, New York **1990**, pp. 908–909.
- Independent recording of the CV of an aromatic imide group revealed a reduction wave at the same reduction potential as the polymer. This indicates that the reduction happens on the side chain.
- D. M. Welsh, A. Kumar, E. W. Meijer, J. R. Reynolds, *Adv. Mater.* **1999**, *11*, 1379.

## Patterned Microstructures of Porous Silicon by Dry-Removal Soft Lithography

By Donald J. Sirbulu, Geoffrey M. Lowman, Brian Scott, Galen D. Stucky, and Steven K. Buratto\*

Luminescent nanoporous silicon remains a broadly studied material due to its potential as an active component in optical or optoelectronic devices.<sup>[1,2]</sup> Recently, applications in sensor devices<sup>[3]</sup> and biomaterials<sup>[4]</sup> have fueled research into ways to controllably pattern the morphology of porous silicon (PSi) thin films. One route to patterned microstructured materials that has shown wide relevance is the family of microcontact printing techniques, collectively known as soft lithography.<sup>[5,6]</sup>

\*] Prof. S. K. Buratto, D. J. Sirbulu, G. M. Lowman, B. Scott, Prof. G. D. Stucky  
Department of Chemistry and Biochemistry  
University of California  
Santa Barbara, CA 93106-9510 (USA)  
E-mail: buratto@chem.ucsb.edu